Communications: SIF Congress 2011

Measurement of the production cross-section ratio of the charmonium states χ_{c2} and χ_{c1} in proton-proton collisions at 7 TeV with CMS

E. Usai

Università di Torino and INFN, Sezione di Torino - Torino, Italy

Summary. — This paper presents the observation of the χ_c resonances and the techniques for the measurement of the $\sigma(pp \to \chi_{c2} + X)/\sigma(pp \to \chi_{c1} + X)$ ratio with the CMS detector at LHC. The measurement was performed with 4.0 fb^{-1} of pp collisions at $\sqrt{s} = 7$ TeV collected in 2011. The χ_c mesons are observed through their radiative decay $\chi_c \to J/\psi \gamma$. The J/ψ were reconstructed through their $\mu^+\mu^-$ decay while the photons were reconstructed through conversions in e^+e^- pairs in the CMS inner tracker. The kinematic range covered is $|y_{J/\psi}| < 1$, 7 GeV/c $< p_{T\,J/\psi} < 25$ GeV/c and $E_\gamma > 0.5$ GeV. Thanks to the excellent performance of the CMS tracking system, a very good separation between the two resonances is achieved.

PACS 13.20.Gd – Decays of J/ψ, Υ, and other quarkonia.
PACS 14.40.Pq – Heavy quarkonia.
PACS 12.38.Qk – Experimental tests.

1. – The χ_c states and motivation for the analysis

The χ_{c0}, χ_{c1} and χ_{c2} are ^3P_J states of charmonium. They were first discovered in radiative decays from the $\psi(3686)$ [1]. They decay radiatively to the $J/\psi(3097)$. Properties of χ_c states are shown in table I.

The mass difference between χ_{c1} and χ_{c2} is only about 45 MeV/c^2 thus separating the two resonances requires a very good resolution of the detector. On the other hand, the χ_{c0} has a low branching fraction in the radiative decay which makes its detection in this channel difficult.

It is known that a significant contribution of J/ψ production is indirect, resulting from decay of higher mass states. In particular, the radiative decay of the χ_{cJ} states accounts for a significant fraction (~ 30–40%) of the prompt J/ψ production seen in hadronic collisions. Therefore any calculation of J/ψ production must include χ_{cJ} production as well. This is one of the reasons why the study of χ_{cJ} resonances is relevant.

TABLE I. – *χ_c states properties.*

Resonance	I^G	J^{PC}	Mass (MeV/c^2)	BR($\chi_c \to J/\psi + \gamma$)	$\Delta m(\chi_c, J/\psi)$ (MeV/c^2)
$\chi_{c0}(1P)$	0^+	0^{++}	3414.75 ± 0.31	$1.14 \pm 0.08\%$	317.8
$\chi_{c1}(1P)$	0^+	1^{++}	3510.66 ± 0.07	$34.1 \pm 1.5\%$	413.7
$\chi_{c2}(1P)$	0^+	2^{++}	3556.20 ± 0.09	$19.4 \pm 0.8\%$	459.3

The measurement of the ratio $\sigma(pp \to \chi_{c2} + X)/\sigma(pp \to \chi_{c1} + X)$ represents also a benchmark for QCD theoretical models on meson production and decays such as Color Singlet Model and NLO corrections to NRQCD calculations.

The cross-section ratio measurement at LHC is not affected by the quark masses or the value of α_s, that cancel out. Similarly, the measurement is unaffected by most experimental acceptance and efficiency factors, that give rise to small corrections except for potentially large effects connected to the unknown spin alignment.

The CMS detector and subdetector technical details are described in [2] and [3].

2. – Analysis strategy

$\chi_{c1,c2}$ candidates are selected by searching for their radiative decays into the $J/\psi + \gamma$ final state, with the J/ψ decaying into two muons. An accurate reconstruction of the photon is then needed to finalize the reconstruction of the χ_c with sufficient resolution. In the center of mass of the charmonium states, the photon has an energy of $413\,\mathrm{MeV}$ when emitted by the χ_{c1} and of $459\,\mathrm{MeV}$ when emitted by the χ_{c2}, which results in a p_T of the photon to be measured mostly between 0.5 and $6\,\mathrm{GeV}/c$ in the laboratory frame. A calorimetric measurement of the photon energy would not provide sufficient resolution to disentangle the two states, whose masses differ by only $45\,\mathrm{MeV}/c^2$. On the contrary, a measurement of the momentum of the electron-positron pair originating from a conversion of the photon, in the beam pipe or in the inner layers of the Tracker, results in a sufficiently accurate measurement of the photon energy. The drawback is the reduced yield due to the small probability for a conversion to occur in the innermost part of the tracker detector and, mostly, to the low reconstruction efficiency.

For each $\chi_{c1,c2}$ candidate, the mass difference $m_{\mu\mu\gamma} - m_{\mu\mu}$ is evaluated. The use of the mass difference reduces the uncertainty to the finite resolution of the e^+e^- pair and avoids the need to constrain the muon pair mass to the J/ψ mass. An unbinned maximum likelihood fit to the mass difference spectrum is performed to extract the yield of χ_{c1} and χ_{c2} as a function of the p_T of the J/ψ. A correction has been applied for the different acceptance of the detector for the two states. The ratio of the production cross-section is then obtained as

$$(1) \qquad \frac{\sigma(pp \to \chi_{c2} + X)}{\sigma(pp \to \chi_{c1} + X)} = \frac{N_{\chi_{c2}}}{N_{\chi_{c1}}} \cdot \frac{\varepsilon_1}{\varepsilon_2} \cdot \frac{\mathrm{BR}(\chi_{c1} \to J/\psi\gamma)}{\mathrm{BR}(\chi_{c2} \to J/\psi\gamma)},$$

where N_{χ_i} is the number of candidates of each type obtained from the fit, $\varepsilon_1/\varepsilon_2$ is the ratio of detection efficiencies for the two states, derived from a full detector simulation and the branching ratios are taken from the PDG [4].
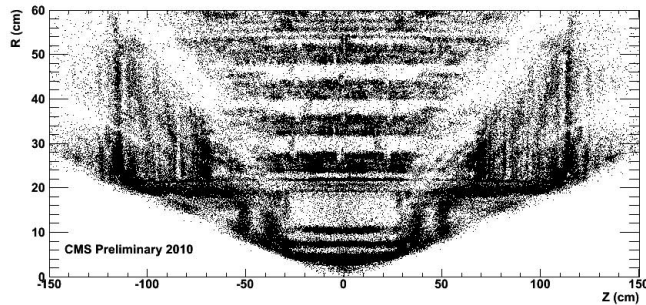
Fig. 1. – Conversion vertices in data in the (z, R)-plane for $|z| < 26$ cm [6].

3. – Event selection

The muon system tracks are required to pass the following requirements: they must have at least 10 hits in the tracker, of which not less than two have to be in the pixel layers, a χ^2 per degree of freedom smaller than 1.8, and must intercept a cylinder of radius 3 cm and length 30 cm centered at the primary interaction vertex with the axis parallel to the beam line.

The two muon trajectories are fitted with a common vertex constraint, and events are retained if the fit χ^2-probability is larger than 1%. In order to restrict the measurement to the prompt signal component, the decay length of the J/ψ is required to be less than 100 μm.

For the χ_{c1} and χ_{c2} selection a J/ψ candidate in the mass range between 3.0 and 3.2 GeV/c^2 is required. The rapidity of the muon pair must be in the interval between -1 and 1. The selection is finalized by several requirements made on the photon conversion reconstruction and selection. Photon conversions are characterized by an electron-positron pair originating from the conversion vertex. The e^+e^- invariant mass must be consistent with zero and the two tracks are therefore parallel at the conversion vertex.

Because of the low energy of photons originating from the radiative decay of the χ_c, the electron and positron resulting from any photon conversion have low momentum and can be only reconstructed within the tracking detector. The tracker-driven conversion reconstruction algorithm is described in detail in [5] and in [6]. The distribution of conversion vertices in the detector is shown in fig. 1.

Here the most important selection criteria are summarized along with further requirements needed to specialize the tracker conversion reconstruction to the χ_c case. Opposite-sign track pairs are required to satisfy basic quality criteria, i.e. have more than four hits and a normalised χ^2 less than 10, additional cuts to reject fake pairs are performed.

Track pairs passing the selection are then fitted to a common constrained kinematic vertex fitter. The 3D constraints imposes the tracks to be parallel in both transverse and longitudinal planes. The pair is retained if the fit converges and its χ^2 probability is greater than 5×10^{-4}.

A reconstructed primary vertex is assigned to the reconstructed conversion by extrapolating the photon momentum and by choosing the closest vertex. If the distance is larger than ten standard deviations, the conversion is rejected. The primary vertex associated to the conversion is required to be compatible with the reconstructed J/ψ vertex. This requirement is fullfilled when the three-dimensional distance between the two vertices is compatible with zero within five standard deviations. Furthermore, a check is done to avoid that the either of the two muon tracks used to define the J/ψ vertex can be used
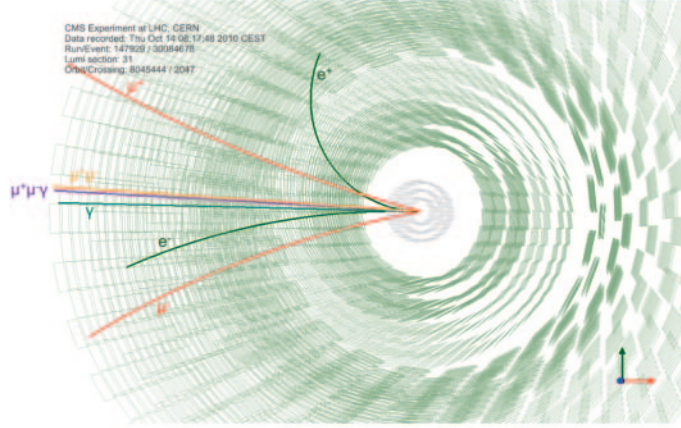
Fig. 2. – Event display of a χ_c candidate [7].

as candidate electron or positron to reconstruct the conversion vertex.

Finally each conversion candidate is associated to every other conversion candidate in the event, and to any photon reconstructed in the Electromagnetic Calorimeter. Any conversion building up a pair which invariant mass falls in the range between 0.08 and $0.20 \, \text{GeV}/c^2$ is rejected, since it assumed to be compatible with a π^0 decay photon. An event display of a χ_c candidate is shown in fig. 2.

4. – Data analysis

To extract the number of χ_{c1} and χ_{c2} from data, an unbinned likelihood fit to the mass difference spectrum is performed in various p_T ranges using RooFit. The signal is modeled using a superposition of three Crystal Ball functions for χ_{c0}, χ_{c1} and χ_{c2}.

$$(2) \qquad f_{\text{CB}}(m) = \begin{cases} e^{-\frac{(m-m_0)^2}{2\sigma}}, & \text{for } \frac{m-m_0}{\sigma} > \alpha, \\ (n/\alpha)^n e^{-\alpha^2/2} \left(\frac{n}{\alpha} - \alpha - \frac{m-m_0}{\sigma} \right)^{-n}, & \text{for } \frac{m-m_0}{\sigma} \leq \alpha. \end{cases}$$

Each Crystal Ball function has four parameters: α, n, σ and m. Due to the small intrinsic width of the states investigated, the observed signal shape is dominated by the experimental resolution. The same α, n and σ is assigned to all three resonance shapes. The m parameter for the χ_{c1} is left free, the masses of the χ_{c2} and χ_{c0} are fixed to the mass differences with respect to the mass of the χ_{c1} through the mass differences reported in the PDG. Hence

$$(3) \qquad m(\chi_{c2}) = m(\chi_{c1}) + (m_{\text{PDG}}(\chi_{c2}) - m_{\text{PDG}}(\chi_{c1})),$$

where $m(\chi_{c2})$ is the free fit parameter and $m_{\text{PDG}}(\chi_{c2}) - m_{\text{PDG}}(\chi_{c1})$ is the mass difference of the PDG.

The combinatorial background is modelled by a probability distribution function of the kind

$$(4) \qquad N_{\text{bkg}} = (x - q_0)^{\alpha_1} \cdot e^{(x-q_0) \cdot \beta_1}$$

where α_1 and β_1 are free parameters and q_0 is fixed to $3.2 \, \text{GeV}/c$. In fig. 3 the measured mass difference spectrum for $p_T^{J/\psi}$ between $7 \, \text{GeV}/c$ and $25 \, \text{GeV}/c$ is shown. This procedure is repeated for several ranges of p_T of the J/ψ in order to extract $N_{\chi_{c1}}$ and $N_{\chi_{c2}}$.
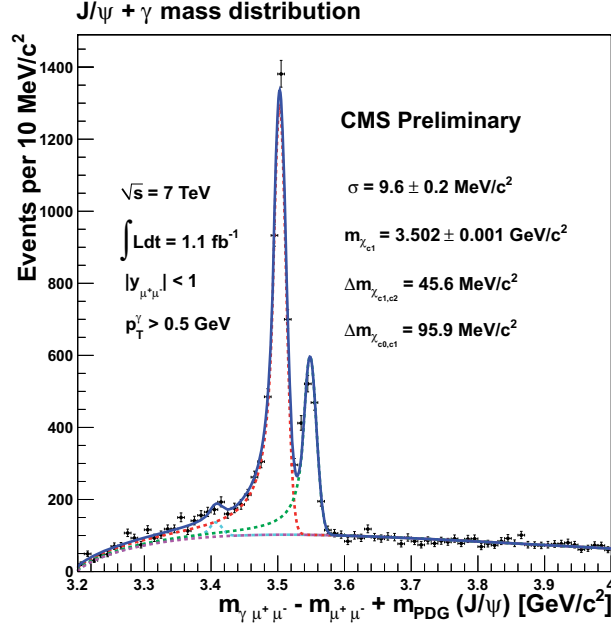
Fig. 3. – Mass difference spectrum for χ_c candidates with $p_T^{J/\psi}$ between $7.0\,\mathrm{GeV}/c$ and $25.0\,\mathrm{GeV}/c$ and $1.1\,\mathrm{fb}^{-1}$ of data [8].

5. – Acceptances and efficiencies

In the calculation of the ratio, the possibility that the geometric acceptance, the photon conversion probability and the reconstruction efficiency are not the same for χ_{c1} and χ_{c2} must be taken into account.

In order to determine the acceptance corrections, a Monte Carlo simulation sample of equal numbers of χ_{c1} and χ_{c2} has been used. This sample was produced by using a PYTHIA particle gun configured in such a way the χ_{c1} and χ_{c2} particles are generated with the same p_T spectrum measured for the prompt J/ψ production. Both χ_c states are forced to decay to $J/\psi + \gamma$. The decay products are then processed through the full CMS detector simulation, trigger selection and reconstruction. In order to increase computational efficiency, only events in which a conversion occurs are passed to trigger emulation and reconstruction.

The ratio of efficiencies for the different bins of p_T of the J/ψ, is obtained as

$$(5) \qquad \frac{\varepsilon_1}{\varepsilon_2}\left(p_T^{J/\psi}\right) = \frac{N_{\chi_{c1}}^{\mathrm{rec}}}{N_{\chi_{c1}}^{\mathrm{gen}}} \cdot \frac{N_{\chi_{c2}}^{\mathrm{rec}}}{N_{\chi_{c2}}^{\mathrm{gen}}} ,$$

where N^{rec} is the number of candidates reconstructed with the selection above, and N^{gen} is the number of candidates generated in the Monte Carlo simulation in the kinematic range $|y^{J/\psi}| < 1.0$, $p_T^\gamma > 0.5\,\mathrm{GeV}/c$. 30 million events have been produced, resulting in about 100000 reconstructed χ_c. The Monte Carlo simulation shows that the ratio $\varepsilon_1/\varepsilon_2$ is close to 1 and does not show a significant dependence on p_T.

The ratio $\varepsilon_1/\varepsilon_2$, which is actually the ratio of the geometric acceptances times the

ratio of the reconstruction efficiencies, is be influenced by: the different acceptance for the muon pair originating from the J/ψ resulting from the decay of the χ_{c1} or the χ_{c2}; the different p_T spectrum of the emitted photon.

The particle gun method allows large samples of χ_{c1} and χ_{c2} to be generated, but in idealized conditions, since the sample is completely free of background. As a consistency check, a PYTHIA sample has been generated on purpose, in which the entire pp collision is reproduced. This "Full Monte Carlo" sample is useful for systematic error studies.

6. – Systematics

Several types of systematic uncertainties are addressed. In particular there are effects that could influence the measurement of the number of χ_{c1} and χ_{c2} from data, the evaluation of $\varepsilon_1/\varepsilon_2$ from the Monte Carlo simulation, and the derivation of the ratio.

Here is a brief summary of the different sources of systematic error considered:

– Choice of fit functional form: the ratio could be affected by a fit function and procedure. The use of two alternative background parametrizations, a polynomial function and a Chebichev function is explored to estimate the possible systematic error.

– χ_{c1}/χ_{c2} counting accuracy: the assumption of different experiment resolution for the χ_{c1} and χ_{c2}, implemented by introducing a free parameter σ_2 for the Crystal Ball describing the χ_{c2} is considered.

– Full simulation *vs.* particle gun: the χ_c particle gun simulation method represent an idealized and somewhat unrealistic situation where there is no background from the other partons involved in the collision. Thus this approach must be validated against a full Montecarlo simulation sample.

– Detector material: since the method presented here relies on photon conversions, the effect of a possible incorrect simulation of the tracker detector material is estimated. Two modified material scenarios, *i.e.* special detector geometries prepared on purpose, have been used to produce as many particle gun Monte Carlo simulation samples. These scenarios correspond to the minimal and maximal increase of the average radiation length, $X_0^{\min}$ and $X_0^{\max}$, respectively, in the hypothesis that 5% in mass of the tracker passive material is not represented in the simulation.

– χ_{c1} and χ_{c2} generated p_T: the effect of assuming in the χ_c gun that the χ_{c1} and χ_{c2} have the same p_T distribution as the J/ψ has been evaluated. The p_T spectrum of the ψ' has been measured and a special Monte Carlo simulation sample in which the χ_c has the same p_T spectrum of the ψ' has been produced.

– Pileup: another possible systematic effect might come from pileup. The 2011 run was characterized by different periods with increasing instantaneous luminosity, leading to a different average number of primary vertices per bunch crossing. The stability of the analysis as a function of the number of primary vertices in the event has been investigated.

– Polarization: the polarization of the χ_{c1} and χ_{c2} is unknown and another possible source of uncertainty. The different angular distribution of the photon may affect the photon p_T distribution, and, taken into account the photon detection

efficiency, the total yield. A standalone Monte Carlo simulation code that features the production χ_{c1} and χ_{c2} in any polarization state is used to estimate the size of this uncertainty, in particular to study the relative variation of $\varepsilon_1/\varepsilon_2$ with different polarization scenarios.

– Branching fractions: the quantity directly accessible with the experiment is

$$\frac{\sigma(pp \to \chi_{c2} + X)}{\sigma(pp \to \chi_{c1} + X)} \times \frac{\mathrm{BR}(\chi_{c2} \to J/\psi + \gamma)}{\mathrm{BR}(\chi_{c1} \to J/\psi + \gamma)}.$$

In order to extract the ratio of the production cross-sections, the value of 1.76 ± 0.10 for $\mathrm{BR}(\chi_{c1} \to J/\psi + \gamma)/\mathrm{BR}(\chi_{c2} \to J/\psi + \gamma)$ is used, as derived from branching ratios with their errors reported in the PDG [4].

7. – Conclusions

Thanks to the excellent performance of the CMS tracking system, a good separation between the two states in the kinematical range $p_T^\gamma > 0.5 \, \mathrm{GeV}/c$, $|y^{J/\psi}| < 1.0$, $p_T^{J/\psi}$ was achieved. In particular the observed width of the χ_c peaks in the mass distribution is lower than $10 \, \mathrm{MeV}/c^2$, which corresponds to the resolution of the inner tracker. This represents a success of the low energy conversion reconstruction algorithm achieved thanks to the robust performance of the inner tracker even in a scenario with low energy tracks and high track multiplicity in the events.

The ratio must be corrected for efficiencies of reconstruction and acceptances. The calculation of the ratio of efficiencies $\varepsilon_1/\varepsilon_2$ is performed through the use of a particle gun Monte Carlo that provides enough statistics to obtain a sufficient precision. Several possible sources of systematics errors have been examined in the analysis.

The study of χ_c states is useful to test theoretical models on quarkonium production and for studies of J/ψ production.

* * *

REFERENCES

[1] KWONG W., ROSNER J. L. and QUIGG C., *Ann. Rev. Nucl. Part. Sci.* (1987).
[2] THE CMS COLLABORATION, *Detector performance and software, Physics Technical Design Report, Vol. I*, CERN/LHC 2006-001, CMS TDR 8.1 (2006).
[3] THE CMS COLLABORATION, *JINST*, **3** (2008) S08004.
[4] NAKAMURA K. *et al.* (PARTICLE DATA GROUP), *J. Phys. G*, **37** (2010) 075021.
[5] THE CMS COLLABORATION, *Tracking and Vertexing Results from First Collisions*, CMS-PAS-TRK-10-001 (2010).
[6] THE CMS COLLABORATION, *Studies of Tracker Material*, CMS-PAS-TRK-10-003 (2010).
[7] THE CMS COLLABORATION, *Observation of the χ_{c1} and χ_{c2} states*, CMS-DP-2011-006 (2011).
[8] THE CMS COLLABORATION, *Observation of the χ_c states with $1.1 \, \mathrm{fb}^{-1}$*, CMS-DP-2011-011 (2011).